International Journal of Engineering and Technology Innovation, vol. 6, no. 4, 2016, pp. 284 - 295

# Influence of Charge Shape and Orientation on the Response of Steel-Concrete Composite Panels

Abraham Christian*, Lado Riannevo Chandra, Satadru Das Adhikary, Khim Chye Gary Ong

National University of Singapore, 1 Engineering Drive 2, Singapore 117576, Singapore.

Received 05 June 2016; received in revised form 15 August 2016; accepted 17 August 2016

## Abstract

Blast design codes usually generalize the shape of the charge as spherical or hemispherical. However, it was found that the blast overpressure of cylindrical charges differ greatly when compared with relevant analytical results generated with the charges assumed to be spherical. The objective is to use fully coupled 3D multi-material arbitrary Lagrangian Eulerian (MMALE) modelling technique in LS Dyna software to simulate the cylindrical charge blast loading. Comparison of spherical and cylindrical charge blast simulation was carried out to show the influence on peak overpressure and total impulse. Two steel-concrete composite specimens were subjected to blast testing under cylinder charges for benchmarking against numerical results. It was found that top detonated, vertical cylinder charge could give much higher blast loading compared to horizontal cylinder charge. The MMALE simulation could generate the pressure loading of various charge shape and orientation to be used for predicting the response of the composite panel.

**Keywords:** blast, charge shape, MM-ALE, steel-concrete composite

## 1. Introduction

Typical blast results, both experimental and numerical, as presented in many scientific papers usually provide details on the nature, mass and stand-off distance of the explosives used. However, the shape of the charge and the location of the detonator are rarely mentioned due to the assumption that eventually the blast wave shape transition into one typical of equivalent spherical or hemispherical charges. This approximation may be acceptable when the distance of interest is large (typically $Z > 4$ to 5 $m/kg^{1/3}$ [1] or greater than 3 $m/kg^{1/3}$ [2]). Nevertheless, it has been reported that the shape and orientation of the charge has considerable effect in close range blast scenarios, resulting in significant differences with regards to the predicted and measured pressures [3-5].

Current standards for blast-resistant design of buildings, e.g. UFC-3-340-02 [6] assume that the charge is spherical and ignore the effect of charge shape. Predictions performed using the UFC-3-340-02 underestimates the reflected overpressures when the charge is cylindrical and oriented vertically. However, the reflected overpressure is overestimated when the charge is either spherical or cylindrical, and in the latter oriented horizontally. For cylindrical charges, the ratio of charge length (L) to diameter (D) affects the pressure distribution and impulse in the immediate vicinity of the explosive; for large values of L/D, most of the energy is directed in the radial direction whereas for small values of L/D, and most of the energy is directed in the axial direction [5].

* Corresponding author. E-mail address: abraham.chr@nus.edu.sg

Esparza [7] compiled a comprehensive review with additional analyses and presented a set of diagrams which may be used to determine the equivalent spherical charge weights when cylindrical charges are used. The results, in the form of multi parameter curve fits, relate the ultimate reflected pressure to the scaled distance Z, to the L/D ratio and the azimuth angle θ (the angle between the longitudinal axis of the cylindrical charge and the measurement axis). However, the graphs are presented for scaled distances > 0.8 kg/m$^{1/3}$.

In another study by Adamik and Vagenknetch [8], numerical 3D simulation techniques for cylindrical shaped TNT charge were outlined. A simplified formula for various orientations of the charges have been developed, thus making it possible to represent the original cylindrical charges as equivalent 3D ellipsoids. However, this technique only applies to the Multi-Material Arbitrary Lagrangian Eulerian (MMALE) method which is very inefficient computationally due to the requirement of modelling the surrounding air element using a fine mesh to achieve acceptable accuracy.

Because of the above, reference values and formulae for the prediction of the peak overpressure, positive impulse, reflected blast waves, etc. initially developed for spherical and hemispherical charges, are unreliable for use with other charge shapes. Extensive study of various other charge shapes has been carried out [1, 3], but thus far none of the blast design codes have incorporated any of the recommendations, especially for close-in blasts. A knowledge of the charge shape effects may be very important in arriving at an accurate estimate of the actual effect associated with a non-spherical vis-à-vis a spherical charge of the same charge weight.

To demonstrate the effect of TNT shape and charge orientation on the blast pressure curve, numerical study of similar charge weight spherical and cylindrical (L/D = 1/2) charges has been performed. The cylindrical charge was positioned in two orientations; vertical orientation (i.e. the axis of the cylindrical charge was perpendicular to the longitudinal axis of the target structure) and horizontal orientation (i.e. the axis of the cylindrical charge was parallel to the longitudinal axis of target structure). LS Dyna MMALE method was employed to predict the blast pressure field to be coupled to the composite panel model. Fig. 1 shows the three shapes of the TNT charge used in the numerical study.

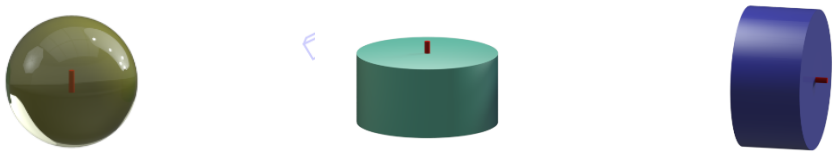

(a) Spherical shape (b) Cylinder shape (vertical) (c) Cylinder shape (horizontal)

Fig. 1 TNT charges with set detonator (red point)

## 2. Simulation of Blast Charges

The blast wave patterns in the vicinity of the cylindrical shaped charge after ignition are different vis-a-vis spherical charges. Thus, the blast wave parameters (positive ultimate overpressure, duration and the positive impulse) cannot be generalized as a spherical charges. The LS Dyna MMALE simulation could show the differences in the pressure fields of a 5kg center detonated spherical charge, a top detonated vertically oriented cylindrical charge and a side detonated horizontally orientated cylindrical charge (Fig. 2). In this 3D MMALE simulation, Jones Wilkins Lee (JWL) TNT properties was used [9] with ¼ symmetry model of size 1200 mm x1200 mm x1200 mm, with a 5mm mesh size air domain. The pressure tracer point was placed at the center of incident face of a rigid steel plate with a 1 meter stand-off distance (SoD)

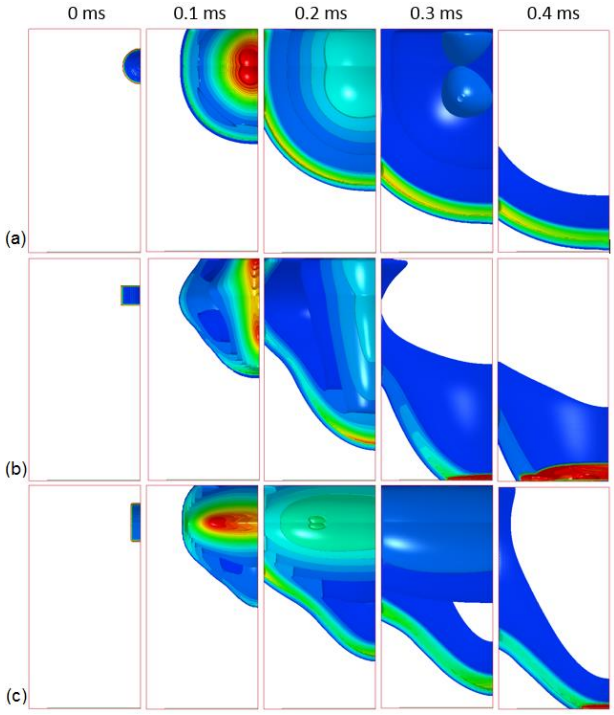


(a) Center detonated spherical charge, (b) Top detonated vertically oriented cylindrical charge, and (c) Side detonated horizontally oriented cylindrical charge

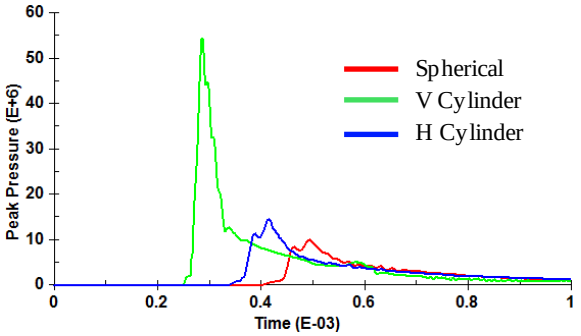


(d) Peak reflected pressure at Z = 0.59

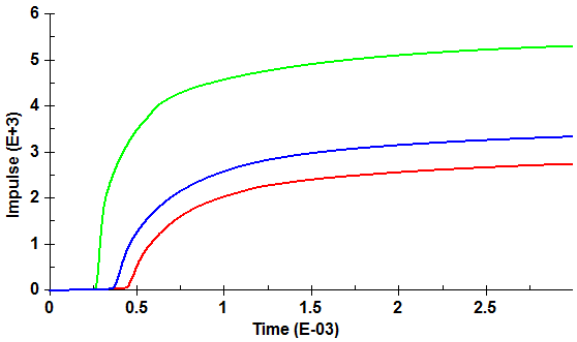


(e) Total impulse at Z = 0.59

Fig. 2 Pressure field comparison of 5 kg TNT

The expansion of the 5kg TNT with different charge shape and orientation can be observed in Fig. 2 (a), (b) and (c). The center detonated spherical charge produced a relatively uniform pressure wave front whereas the top detonated vertically oriented cylindrical charge generated higher energy, shock wave front, showing sharper wave head. As observed, the blast wave arrived earlier than the spherical and horizontally oriented cylindrical charge. The horizontally oriented cylindrical charge pressure field is similar to the vertically oriented cylindrical charge. Only the orientation differed by 90 degrees. Neverth eless, the shock wave front still arrived earlier than that of the spherical charge. This means that the blast energy from the side of cylindrical charge is higher compared to that of the spherical uniform wave front.

As can be seen in Figs. 2 (d) and 2(e), it is clear that the top detonated vertically oriented cylindrical charge delivered the highest peak pressure and total impulse at the center of the incident face of the steel plate. With the same charge weight of 5 kg, the top detonated vertically oriented cylindrical charge produced almost six times the peak pressure and twice the total impulse vis-à-vis a center detonated spherical charge. The horizontally oriented cylindrical charge showed slight pressure and impulse differences (1.4 times the pressure and 1.2 times the impulse) vis-à-vis the spherical charge. This MMALE simulation showed that the loading imparted to the target structure can be significantly different when using cylindrically shaped charges, esp ecially if they are oriented vertically and detonated at the top.

The mass equivalent plots for cylindrical charges from Esparza [7] indicated that the generated over pressure could be more than ten times the over pressure generated from a spherical charge of the same mass. In the case of a vertically oriented cylindrical charge (Fig. 3 (a)), the ratio of the overpressure generated at the center to that at the side of the target panel is way beyond the graph Z ratio (hence, the ratio may be more than 10), whereas a horizontally oriented cylindrical charge (Fig. 3 (b)) only produced an ave rage of 0.85 times the peak pressure generated by a spherical charge. This clearly s howed the huge difference that is expected caused solely by the orientation of the cylindrical charge.

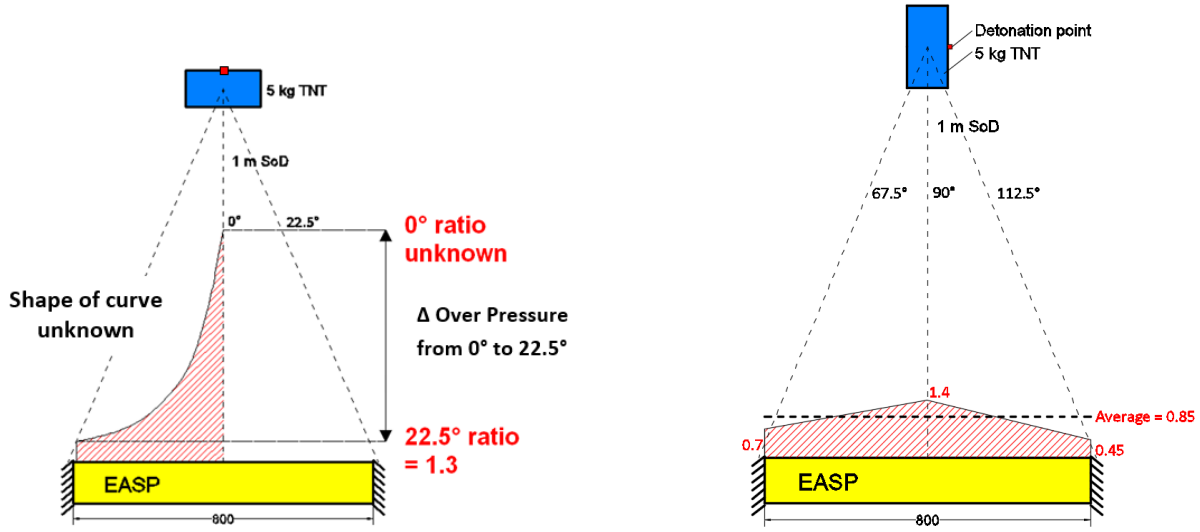


(a) Top detonated vertically oriented cylindrical charge (b) Side detonated horizontal cylinder charge

Fig. 3 Blast pressure predicted for a cylindrical charge of the equal mass as a spherical one [7]

During the course of testing, it was observed that the blast overpressure of the two blast tests differ greatly when compared with respective results obtained analytically based on modelling the charges as spherical charges. This was especially evident in the case when the charge was placed in the vertical direction. Further analysis of the EASP1-C110F (specimens based on Fig. 4), blast experimental results obtained seemed to suggest that the blast loading seems to be localized in the middle portion of the test specimen. This was subsequently confirmed as reported by literature on cylinder blast pressure generation [8]. It was for this reason that midway through this series of blast tests, the decision was made to change the orientation of the charge from a perpendicular charge placement configuration to a parallel one for the EASP1-C110 specimen.

## 3. Blast Tests Conducted On Steel-Concrete Composite Panels

The novel composite panel combines a fiber reinforced high strength concrete panel as the receptor layer with a steel sandwich panel as the second layer. The latter serves as an energy absorption medium through deformability of its sandwich structure, and provides protection against fragmentation of the concrete present in the receptor layer. However, this paper mainly focuses on investigating the response of the concrete steel composite panels named Energy Absorption Sandwich Panel (EASP) designed as sacrificial cladding panel subjected to vertical and horizontal cylindrical charge shape blast loading.

Fabrication of the EASP begins with the steel sandwich assembly to be used as formwork to cast the concrete layer. The interface and distal, 2 mm thick steel plates were perforated with a series of alternating slots made by a laser cutting machine and welded to the protruding core plates using the manual metal inert gas (MIG) welding process. Slot joints were designed to facilitate assembly of the interface and distal steel plates and the core plates of the sandwich layer via slotting before welding commences.

Steel-concrete composite panel specimens (EASP1, see [10] for further details) of dimensions of 800 mm x 300 mm x 110 mm (span length x width x depth) were cast with either high strength concrete (HSC) C110 (f'c = 145 MPa) or fiber reinforced high strength concrete (FRHSC) C110F (f'c = 131.5 MPa) as the concrete layer. For the concrete and fiber reinforced cementitious mixtures, ASTM Type I normal OPC was used. Densified silica fume with a specific gravity of 2.2 was also used. Coarse aggregates with maximum size of 10 mm was used in all the concrete mixtures. A superplasticizer or High Range Water Reducers (HRWA) admixture was added in the mixtures to achieve the target workability. In the case of the C110 and C110F concrete, owing

to the very low water content and the use of silica fume, additional shrinkage reducing admixture (SRA) was used to replace 3% of the water as required. Straight high carbon steel wire fibers, 0.16 mm diameter and 13 mm long, were used in the C110F mix (0.5% by weight). The mix designs based on 0.95% sand/water content are summarized in Table 1.

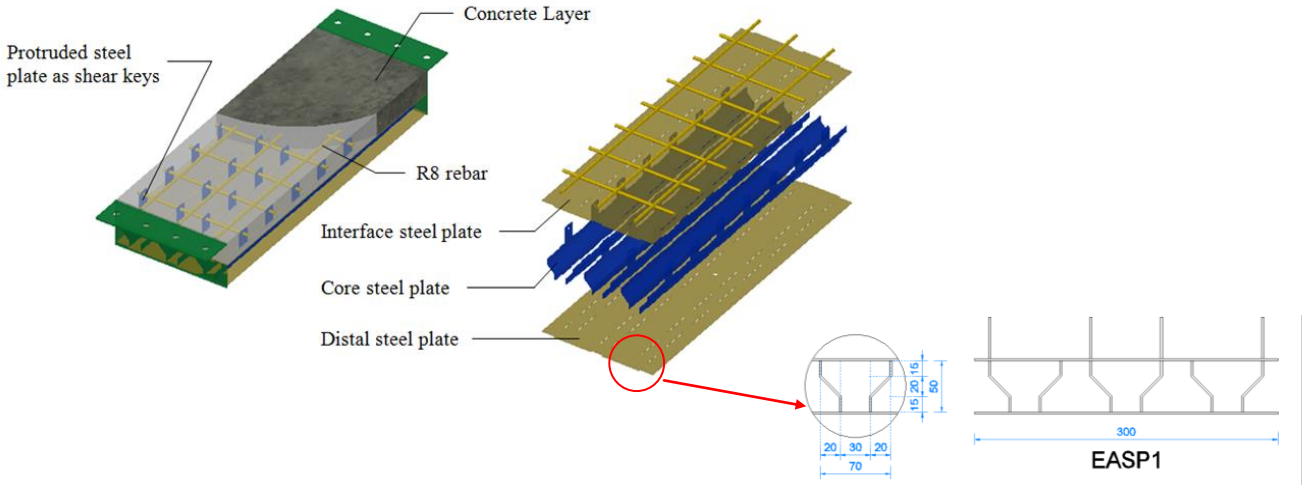


Fig. 4 Steel-concrete composite panel specimens (EASP1)

Table 1 Concrete Mix Design (per $m^3$)

| Specimen | w/c | Cement(kg) | SF(kg) | Water(ltr) | CA(kg) | Sand(kg) | SP(ltr) | SRA(ltr) | Steel Fiber(kg) |
|---|---|---|---|---|---|---|---|---|---|
| C110 | 0.31 | 450 | 45 | 139 | 946 | 798 | 5.5 | 4.17 | - |
| C110F | 0.30 | 450 | 45 | 135 | 946 | 772 | 6.7 | 4.38 | 39 |

The panels were subjected to 5 kg cylindrical shaped explosives with a L/D length ratio of 1:2 placed centrally at mid-span with 1m standoff distance. The TNT charge was supported by a light wooden frame support as shown in Fig. 5 (a), (b). The test specimens were fixed to the rigid steel frame support using bolts connection (Fig. 5 (c)).

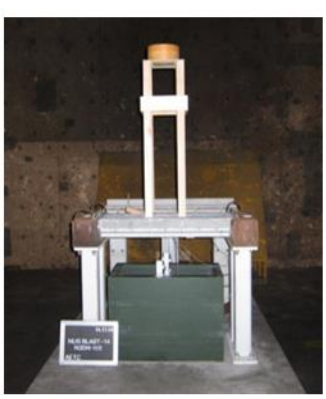

(a) EASP1-C110F composite panel

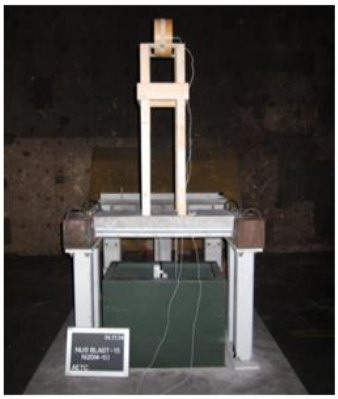

(b) EASP1-C110 composite panel

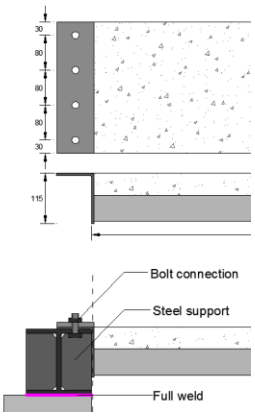


(c) Fixed end connection of both blast test

Fig. 5 Blast test set-up

The axis of the cylindrical charge was oriented in the vertical direction for the EASP1-C110F specimen and in the horizontal direction for the EASP1-C110 specimen as shown in Fig. 5. The charges were detonated with the aid of a booster charge of higher grade explosive that was attached to the top surface of the cylinder in the case of EASP1-C110F and on the right circular surface in the case of EASP1-C110. Two pressure sensors were placed on each of the two steel supports, located at a distance of 500 mm from the center of the specimen. Unfortunately, due to technical problems, the sensors did not capture the pressure and displacement data as planned. Only maximum and residual deflection could be measured after the blast test to compare with the numerical model.

Due to the relatively short standoff, gases and fire resulting from the TNT explosion affected the panel in addition to air particles. The explosion of the 5kg TNT charge could be observed on the footage of the high-speed video recordings. It could be seen from Figs. 6 and 7 that the TNT explosion generated lots of fire and smoke. The images indicated that there was a jetting effect along the axis of the cylinder. This phenomenon is likely to lead to higher pressures at the center of the specimen especially in the case of C110F specimen for the vertical TNT placement.

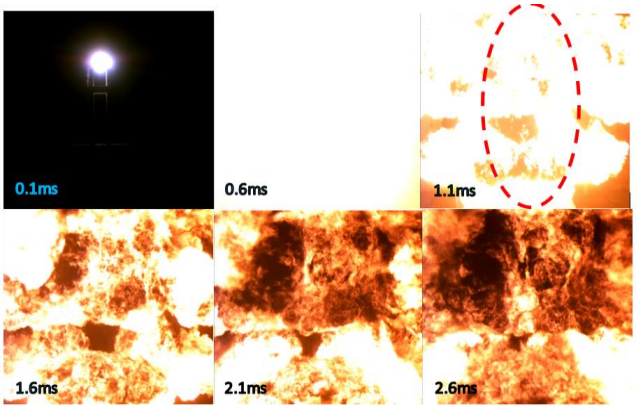


Fig. 6 High speed video footage of 5 kg TNT blast with vertical placement showing marked jetting effects

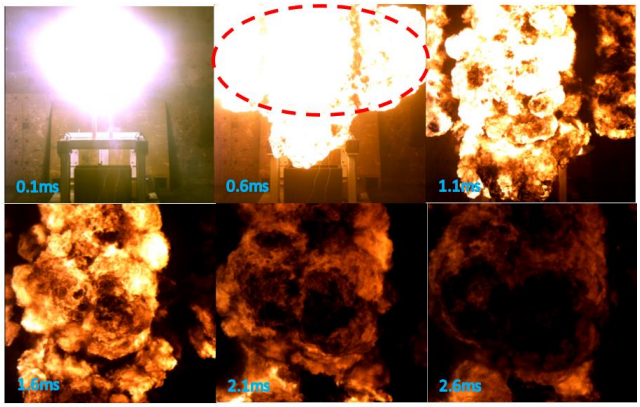


Fig. 7 High speed video footage of 5 kg TNT blast with horizontal placement showing marked jetting effects

The EASP1-C110F specimen registered a maximum deflection of 200 mm (the back of specimen was hitting the sensor holder, hence actual maximum deflection may be more than 200 mm) and residual deflection of 144 mm. The severe damage observed on the EASP1-C110F specimen, significantly larger than that of EASP1-C110, served to confirm the observation made above about the difference between vertically and horizontally oriented cylindrical charges. Not least because EASP1-C110F panel specimen was expected to perform better than the EASP1-C110. The vertically oriented charge, placed at the same distance directly above the center of the panels, clearly resulted higher blast energy upon detonation of the charge, especially within the central portion of the incident face of the EASP1-C110F specimen.

(a) EASP1-C110F (b) EASP1-C110

Fig. 8 Specimens after blast test

The extensive damage of EASP1-C110F specimen can be seen in Fig. 8 (a). Buckling of the steel sandwich core extended well beyond the mid span region of the panel. The concrete layer delaminated fully on one side of the panel with the end plate bent out of shape. The shear connector used was clearly not adequate in maintaining composite action between the concrete and the steel sandwich layer. On the other side of the span, there was also delamination of the concrete layer, without detachment, with relatively less deformation of the end plate. Although the panel experienced severe deformation, it was not breached, and very little concrete spalling was observed. The fiber reinforced concrete presents in the concrete layer seemed to have minimized the propagation of cracks while keeping intact the crushed concrete portions of the concrete layer with minimal concrete spalling and fragmentation. The steel sandwich layer seemed to have absorbed the blast energy primarily through core crushing. The steel rebar attached to the end plate was sheared off and the side steel plate connection separated cleanly from the side cover plate and

was bent out of shape due to the large bending deformation (Fig. 9). It seemed that the connection between edge of the panel and the support plate is inadequate to maintain overall integrity of the steel-concrete composite panel when subjected to blast loading by the vertically oriented cylindrical charge. The failure mode may be characterized as the global failure mode arising from fle xural failure.

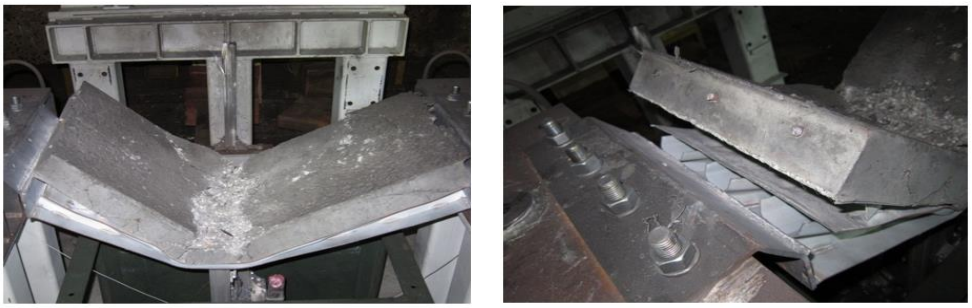

(a) Steel sandwich and concrete crushing (b) Side plate connection failure

Fig. 9 Failure mode of the EASP1-C110F specimen

The EASP1-C110 tested with the parallel charge configuration registered displacements monitored using las er sensors. However, the sensor did not register any value for an initial duration of 58 ms after ignition of the TNT charge. Possible ca uses of this black-out period could be attributed to either the fire or smoke generated or a combination of both during the blast or to the electro-magnetic pulse (EMP) generated during detonation of the TNT charge. Due to the black-out period, lasting for about 58 ms before readings were captured, the maximum displacement was not recorded by the laser sensor. The maximum displacement of the EASP1-C110 specimen was obtained using the plasticine gauge.

The EASP1-C110 specimen failed in shear (Fig. 8 (b)). The failure may be due to the brittleness of high strength concrete. The mode of failure seems similar to that reported by Low and Hao [7] associated with slabs subjected to high blast load amplitude. They suggested that RC slabs tend also to fail in the direct shear mode if it is relatively stiff and with a small span lengt h.

The EASP1-C110 was tested with the horizontally oriented cylindrical charge detonated from the right. The maximum displacement of the EASP1-C110 specimen was 27.5 mm, monitored using plasticine gauges. It can be seen that the EASP1-C110 specimen failed in shear. The failure may be due to the brittleness of high strength concrete without any steel fibers incorporated. The severity of the damage to the concrete and steel sandwich layer is much less compared to the EASP1-C110F specimen although this specimen is expected to perform worse for the same charge weight at the same stand-off distance.

## 4. Coupled MM-ALE Simulation of the Steel-Concrete Composite Panel

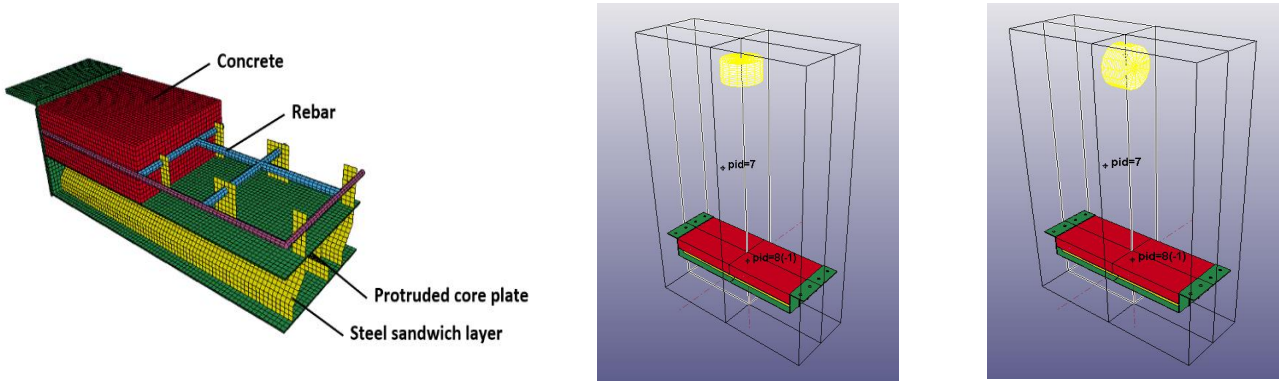


(a) EASP1-C110F (b) EASP1-C110 (c) EASP1-C110 blast setup

Fig. 10 LS Dyna finite element model and setup

The LS Prepost software was employed to develop a 3D quarter scale model by using both X and Y symmetry axes to reduce computational costs. In the EASP1 finite element model, concrete material model used rectangular 8-noded solid elements with a 5 mm mesh size. The rebar inside the concrete was modelled as beam-truss elements capable of resisting only axial forces in tension or compression. The rebar model is then connected to the concrete utilizing common nodes without bond-slip consideration. To model the actual geometry of the cellular steel sandwich using solid elements, a simplified model that combines both solid elements and shell elements were used for the steel sandwich layer. The FE model of the EASP1 specimen is shown in Fig. 10 (a), the simulation setup in Fig. 10 (b) and (c) for EASP C110F and C110, respectively.

Material model 72 Release III (MAT 72R3 - Concrete Damage Model) in LS DYNA was utilized to model the concrete layer. The calibration method of the MAT72R3 model for fiber reinforced high strength concrete C110F and high strength concrete C110 involves alteration of the damage scaling exponents, b1 for the unconfined uniaxial stress-strain curve in compression and b2 for the hardening and softening of the unconfined uniaxial tensile stress-strain curve. The steel rebar and steel plate materials utilized MAT3 Plastic Kinematic to model the behavior of steel, including strain rate effects. Hourglass Type 1 and type 6 with a calibrated coefficient was included in the solid element formulation to prevent zero energy modes as well as to control the concrete element erosion. The dynamic increase factor (DIF) for compressive strength and tensile strength used the CEB-FIP (1990) model code [11]. The interaction between separated material nodes was invoked through contact interfaces, automatic surface to surface contact with static and dynamic friction coefficient of 0.57 and 0.45 respectively was used to model the bond behavior at the interface between the steel and concrete materials [12]. In order to model the overlapping welded joints, some connection segments between the interface and distal steel plates of the steel sandwich layer were joined using common nodes for those that are welded and separated for those not welded accordingly. Strain failure is selected as the failure criterion in the concrete erosion parameter because of the relatively high strain rate loading condition. The chosen value of maximum principal strain and minimum principal strain at failure are 0.5 and -0.9 respectively [13].

AA-quarter scale symmetrical model with 5 mm air boundary mesh was constructed for the TNT explosion. The ALE portion defined by *ALE_MULTI_MATERIAL_GROUP keyword, air was defined as MAT9 Null material model with MAT8 High Explosive Burn for the TNT material model [9]. A reference pressure PREF of 101.3 kPa was added to the free side of the air domain to balance the internal pressure. In the MMALE approach, Lagrangian and ALE solution were combined in the same model and the fluid-structure interaction (FSI) handled the coupling algorithm.

The fluid-structure interaction in LS Dyna was modelled with *CONSTRAINED_LAGRANGE_IN_SOLID keyword. Specific donor cell advection method 3 was used to ensure conservation of total energy in the system. The *INITIAL_VOLUME_FRACTION_GEOMETRY card defines the initial distribution of air and TNT, the placement and initial shape of TNT. Card *INITIAL_DETONATION defines where and when the detonation starts.

The results of the EASP1-C110F and EASP1-C110 blast simulation can be seen in Fig. 11 and 12. The numerical prediction of the residual deflection was 131 mm compared to the experimental result of 144 mm. The numerical model under predict the experimental residual displacement due to the advection error of MM-ALE mesh. The steel sandwich layer exhibited core compression failure (indicated by crushed steel sandwich core).

For the blast test conducted on the EASP1-C110 specimen, the damage and the residual deflection of the numerical model agreed well with the actual experimental results (12.6 mm of numerical residual deflection compared to 12.5 mm experimental residual deflection. However, the model under predict the maximum deflection (17.4 mm vs. 27.5 mm). The FE model exhibited concrete erosion near the supports, similar to that observed on the EASP-C110 specimen tested experimentally.

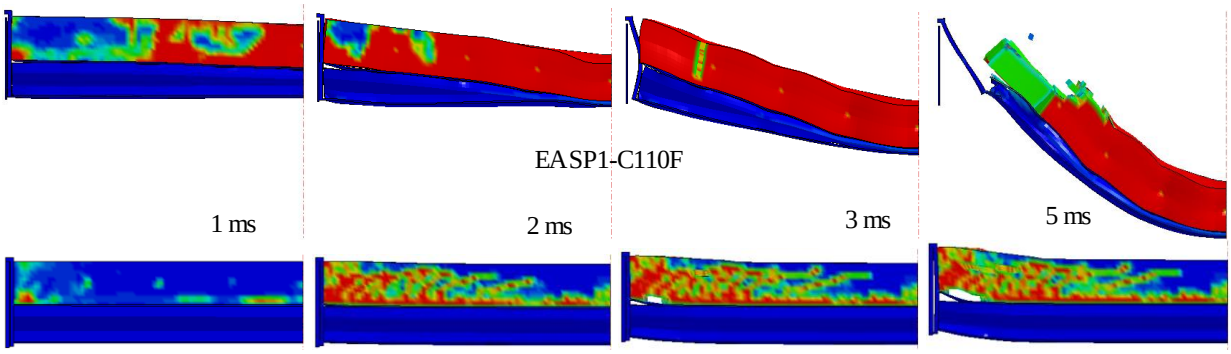


Fig. 11 Finite element model damage progression

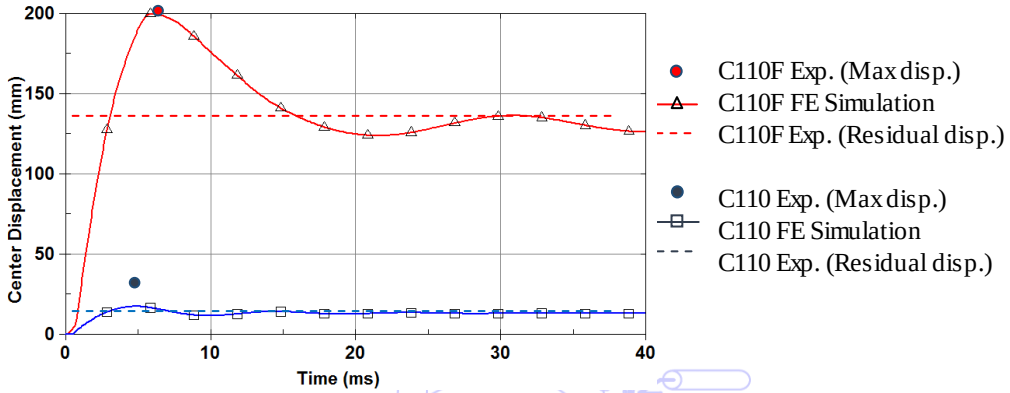


Fig. 12 EASP center displacement (experiment vs. numerical)

## 5. Conclusions

Results obtained based on numerical simulation of various blast charge shape, orientation and detonation point, suggests that the LS Dyna software could model the effect of charge shape to the generated pressure field in close -in explosion. It was found that the top detonated cylindrically shaped charge produced higher peak over pressure compared to a spherical charge of the same charge weight and stand-off distance.

The EASP1 specimens with C110 and C110F concrete were subjected to cylindrically shaped, 5 kg TNT explosion at 1 meter stand-off distance. The EASP1-C110F specimen was tested with a vertical charge orientation resulting in severe concrete and steel sandwich layer damage as well as a large mid-span residual deflection of 144 mm. The results suggest that the actual blast pressure generated experimentally is likely to be more than six times that of a 5 kg spherical charge. Despite the very high blast loading generated from the vertically oriented cylindrical charge, the EASP1-C110F was able to withstand the blast with minimal concrete fragmentation of the concrete layer. It is apparent that combining a receptor layer cast with a fiber reinforced high strength concrete on top of a the cellular steel sandwich layer is efficient in absorbing close-in blast. EASP1-C110 specimen was not damaged as severely as the EASP1-C110F specimen, even though steel fibers were not incorporated in the concrete mix.

It was found that 3D MMALE method could simulate the blast effect of various charge shape and orientation. However, the computational cost is very high due to fine mesh needed to capture useful peak pressure and total impulse arising from the TNT explosion. Currently, this method may be the best option for non-spherical charge simulation, requiring a large number of processing core and memory to reduce computation time. The two blast tests carried out and numerical simulation of EASP1 specimens, showed that the incorporation of a steel sandwich layer behind the concrete receptor layer could contain concrete fragments that are generated during the blast. Further details of the EASP specimens and the their performance against close-in blast and impact loading can be found in reference [14].

## References


[1] B. Simoens and M. H. Lefebvre, "Influence of the shape of an explosive charge: quantification of the modification of the pressure field," Central European Journal of Energetic Materials, vol. 12, pp. 195-213, 2015.

[2] P. Sherkar, J. Shin, A. Whittaker, and A. Aref, "Influence of charge shape and point of detonation on blast-resistant design," Journal of Structural Engineering, vol. 142, p. 04015109, 2016.

[3] M. Ismail and S. Murray, "Study of the blast waves from the explosion of nonspherical charges," Propellants, Explosives, and Pyrotechnics, vol. 18, pp. 132-138, 1993.

[4] B. Simoens, M. H. Lefebvre, and F. Minami, "Influence of different parameters on the TNT-equivalent of an explosion," Central European Journal of Energetic Materials, vol. 8, pp. 53-67, 2011.

[5] C. Wu, G. Fattori, A. Whittaker, and D. J. Oehlers, "Investigation of air-blast effects from spherical-and cylindrical-shaped charges," International Journal of Protective Structures, vol. 1, pp. 345-362, 2010.

[6] UFC3-340-02, "Structures to resist the effects of accidental explosions," Department of the Army and Defense Special Weapons Agency, Washington, DC, USA, 2008.

[7] E. D. Esparza, "Spherical equivalency of cylindrical charges in free-air," presented at the 25th Department of Defense Explosives Safety Seminar, Texas, 1992.

[8] V. Adamik, J. Vagenknetch, P. Vavra, and W. A. Trzcinski, "Effect of TNT charges orientation on generated air blast waves," presented at the ANSYS User's Meeting, Czech Republic, 2004.

[9] E. Lee, M. Finger, and W. Collins, "JWL equation of state coefficients for high explosives," United States, 1973.

[10] A. Christian and K. C. G. Ong, "Performance of fiber reinforced high-strength concrete with steel sandwich composite system as blast mitigation panel," Procedia Engineering, vol. 95, pp. 150-157, 2014.

[11] B. Riisgaard, T. Ngo, P. Mendis, C. T. Georgakis, and H. Stang, "Dynamic increase factors for high-performance concrete in compression using split Hopkinson pressure bar," Fracture Mechanics of Concrete and Concrete Structures, vol. 1-3, pp. 1467-1471, 2007.

[12] B. Rabbat and H. Russell, "Friction coefficient of steel on concrete or grout," Journal of Structural Engineering, vol. 111, pp. 505-515, 1985.

[13] M. J. Islam, Z. S. Liu, and S. Swaddiwudhipong, "Numerical study on concrete penetration/perforation under high velocity impact by ogive-nose steel projectile," Computers and Concrete, vol. 8, pp. 111-123, 2011.

[14] A. Christian, "Fibre reinforced high strength concrete with cellular steel sandwich composite panel for blast and impact mitigation," Ph.D, Civil & Environmental Eng., National University of Singapore, Singapore, 2015.